doi:10.1093/brain/awy242 BRAIN 2018: 141; 2952–2965 | 2952

BRAIN
A JOURNAL OF NEUROLOGY

Evidence for peri-ictal blood–brain barrier dysfunction in patients with epilepsy

Theodor Rüber,[1,*] Bastian David,[1,*] Guido Lüchters,[2] Robert D. Nass,[1] Alon Friedman,[3,4] Rainer Surges,[1,5] Tony Stöcker,[6] Bernd Weber,[1] Ralf Deichmann,[7] Gottfried Schlaug,[8] Elke Hattingen[9] and Christian E. Elger[1]

*These authors contributed equally to this work.

Epilepsy has been associated with a dysfunction of the blood–brain barrier. While there is ample evidence that a dysfunction of the blood–brain barrier contributes to epileptogenesis, blood–brain barrier dysfunction as a consequence of single epileptic seizures has not been systematically investigated. We hypothesized that blood–brain barrier dysfunction is temporally and anatomically associated with epileptic seizures in patients and used a newly-established quantitative MRI protocol to test our hypothesis. Twenty-three patients with epilepsy undergoing inpatient monitoring as part of their presurgical evaluation were included in this study (10 females, mean age ± standard deviation: 28.78 ± 8.45). For each patient, we acquired quantitative T_1 relaxation time maps (qT1) after both ictal and interictal injection of gadolinium-based contrast agent. The postictal enhancement of contrast agent was quantified by subtracting postictal qT1 from interictal qT1 and the resulting ΔqT1 was used as a surrogate imaging marker of peri-ictal blood–brain barrier dysfunction. Additionally, the serum concentrations of MMP9 and S100, both considered biomarkers of blood–brain barrier dysfunction, were assessed in serum samples obtained prior to and after the index seizure. Fifteen patients exhibited secondarily generalized tonic-clonic seizures and eight patients exhibited focal seizures at ictal injection of contrast agent. By comparing ΔqT1 of the generalized tonic-clonic seizures and focal seizures groups, the anatomical association between ictal epileptic activity and postictal enhancement of contrast agent could be probed. The generalized tonic-clonic seizures group showed significantly higher ΔqT1 in the whole brain as compared to the focal seizures group. Specific analysis of scans acquired later than 3 h after the onset of the seizure revealed higher ΔqT1 in the generalized tonic-clonic seizures group as compared to the focal seizures group, which was strictly lateralized to the hemisphere of seizure onset. Both MMP9 and S100 showed a significantly increased postictal concentration. The current study provides evidence for the occurrence of a blood–brain barrier dysfunction, which is temporally and anatomically associated with epileptic seizures. qT1 after ictal contrast agent injection is rendered as valuable imaging marker of seizure-associated blood–brain barrier dysfunction and may be measured hours after the seizure. The observation of the strong anatomical association of peri-ictal blood–brain barrier dysfunction may spark the development of new functional imaging modalities for the *post hoc* visualization of brain areas affected by the seizure.

1 Department of Epileptology, University of Bonn Medical Center, Bonn, Germany
2 Center for Development Research, University of Bonn, Bonn, Germany
3 Department of Medical Neuroscience, Faculty of Medicine, Dalhousie University, Halifax, Canada
4 Departments of Physiology and Cell Biology, Cognitive and Brain Sciences, Zlotowski Center for Neuroscience, Ben-Gurion University of the Negev, Beer-Sheva, Israel
5 Section of Epileptology, Department of Neurology, University Hospital RWTH Aachen, Aachen, Germany
6 German Center for Neurodegenerative Diseases (DZNE), Bonn, Germany
7 Brain Imaging Center, Goethe University Frankfurt, Frankfurt, Germany
8 Stroke Recovery Laboratory, Beth Israel Deaconess Medical Center/Harvard Medical School, Boston, MA, USA
9 Department of Radiology, University of Bonn Medical Center, Bonn, Germany

Received March 13, 2018. Revised July 16, 2018. Accepted August 8, 2018

Correspondence to: Theodor Rüber, MD
Department of Epileptology, University of Bonn Medical Center
Sigmund-Freud-Str. 25, 53127 Bonn, Germany
E-mail: theodor.rueber@ukbonn.de

Keywords: blood–brain barrier; epilepsy; quantitative MRI; seizures; serum markers

Abbreviations: FS = focal seizure; GTCS = generalized tonic-clonic seizure; PVE = partial volume estimate; qT1 = quantitative T_1 relaxation

Introduction

The blood–brain barrier is a highly selective, semipermeable interface regulating the passage of ions and larger molecules into the extracellular matrix of the CNS and thereby playing a crucial role in maintaining strict neuronal homeostasis (Obermeier *et al.*, 2013). The association between epilepsy and the blood–brain barrier has long been suggested (Jasper, 1970); however, epilepsy research has faced a crucial question since then: whether the blood–brain barrier dysfunction is a cause or a consequence of epileptic seizures or both (Friedman, 2012). There is a burgeoning body of evidence including animal and patient studies supporting that a dysfunction of the blood–brain barrier contributes to epileptogenesis (Fieschi *et al.*, 1980; Zappulla *et al.*, 1985*a*, *b*; Seiffert *et al.*, 2004; Ivens *et al.*, 2007; van Vliet *et al.*, 2014, 2016; Weissberg *et al.*, 2015; Bar-Klein *et al.*, 2017). Conversely, blood–brain barrier dysfunction has been suggested to be a consequence of epileptic seizures in animal studies (Roch *et al.*, 2002; Librizzi *et al.*, 2012; Vazana *et al.*, 2016), but evidence remains sparse in animals and is only anecdotally reported in clinical case studies (Horowitz *et al.*, 1992; Hattingen *et al.*, 2008; Alvarez *et al.*, 2010). There is, thus, a lack of knowledge regarding the peri-ictal modulation of blood–brain barrier permeability in patients, which we try to address with the current study. In patients, contrast-enhanced quantitative MRI has been used to interrogate blood–brain barrier permeability and has been widely shown to have a higher diagnostic value than conventional dynamic-contrast enhanced MRI (Hattingen *et al.*, 2013; Jurcoane *et al.*, 2013; Bourcier *et al.*, 2017). The basic approach to quantitative MRI is relaxometry, which directly measures the relaxation time instead of the ill-defined signal intensities of conventional MRI (Deoni, 2010; Margaret Cheng *et al.*, 2012; Hattingen *et al.*, 2015).

In this study, we performed T_1-relaxometry (qT1) at various time points after both ictal and interictal injection of gadolinium contrast agent in epilepsy patients and contrasted the resulting volumes to quantify postictal enhancement. As a complement, we investigated postictal and interictal serum levels of proteins S100 and MMP9, which are both considered indicators of blood–brain barrier dysfunction (Kapural *et al.*, 2002; Barr *et al.*, 2010). Our two hypotheses state that blood–brain barrier dysfunction is temporally associated with single epileptic seizures (peri-ictal) in patients (Hypothesis 1) and that more extended epileptic ictal activity would result in anatomically more widespread blood–brain barrier dysfunction (Hypothesis 2). To test Hypothesis 1, we analysed qT1 scans at different time points after both ictal and interictal injection of contrast agent and examined S100 and MMP9. To test Hypothesis 2, we contrasted the results of patients who showed secondarily generalized tonic-clonic seizures (GTCSs) to the results of patients who exhibited focal seizures. The goal of the current study was to image ictally-associated blood–brain barrier dysfunction in epilepsy patients by using a newly established protocol.

Materials and methods

Study design

Twenty-three patients [10 females; mean age ± standard deviation (SD): 28.78 ± 8.45 years] with medically refractory focal epilepsy and undergoing presurgical evaluation for epilepsy surgery at the Department of Epileptology at the University of Bonn Medical Center were included in the study. The patients were prospectively enrolled after they had been admitted to the video-EEG monitoring unit and met the following inclusion criteria: (i) no contraindications to MRI; (ii) age $\geq$ 18 years; (iii) no mental disability; (iv) no history of allergic reactions to MRI contrast dyes and kidney disease; and (v) serum creatinine $<$ 1 mg/dl. As part of the presurgical evaluation, all patients underwent clinical examinations, video-EEG monitoring including the recording of seizures, neuroradiological MRI, neuropsychological assessment, and routine blood tests. The presumed seizure onset zone was localized based on the summary of all diagnostic results. Nine of 23 patients had no apparent lesion on MRI and were considered magnetic resonance-negative. The presumed seizure onset zone was, in these cases, localized by means of modalities other than MRI. For the purpose of the study, patients underwent a minimum of three MRI sessions: one contrast-enhanced qT1 scan (i.e. T_1 relaxometry) after both ictal and interictal injection of contrast agent, respectively, was conducted additionally to one pre-contrast qT1 scan. Sixteen of 23 patients underwent more than one scan after postictal and interictal injection: seven of these 16 patients underwent two postictal and two interictal qT1 scans. Nine of 16 patients underwent three qT1 scans after both ictal and interictal injection of contrast agent (three postictal and three interictal scans). The injection-to-qT1 time intervals were ensured to be equal for both postictal and interictal scans. Thus, each postictal qT1 volume could be contrasted with interictal qT1 volumes acquired with the same injection-to-qT1 time interval. Interictal qT1 scans were performed a minimum of 2 days after the postictal contrast enhanced qT1-scan and after a clinical seizure-free period of at least 24 h. The pre-contrast qT1 scan was performed at least 2 days after the interictal contrast enhanced qT1 scan and a

Table 1 Overview: subjects and measurements

Patient ID	Gender	Age, years	Duration of seizure, s	Latency of injection, s	Latency of qMRI acquisition, min			Serum sample
					Scan 1	Scan 2	Scan 3	
FS group								
1	M	51	24	10	18	190	–	Yes
2	M	32	30	2	15	–	–	No
3	F	24	236	42	37	310	334	No
4	M	26	33	18	39	210	366	No
5	F	27	23	4	16	262	–	No
6	F	19	33	16	34	200	–	Yes
7	M	35	36	10	266	352	488	Yes
8	M	34	57	12	27	–	–	No
9	F	29	48	6	210	475	–	No
10	M	23	34	17	45	–	–	Yes
11	M	20	32	13	29	241	378	No
12	M	50	36	12	21	–	–	No
13	F	26	77	21	27	–	–	No
14	F	23	39	19	30	228	373	No
15	M	27	40	9	24	–	–	No
GTCS group								
16	M	26	118	38	225	–	–	No
17	M	23	105	24	47	318	450	Yes
18	F	29	91	3	65	254	–	No
19	F	19	60	9	29	181	500	No
20	F	34	72	14	38	154	329	No
21	M	22	74	17	26	106	372	No
22	M	27	92	10	81	266	–	Yes
23	F	36	78	7	259	425	–	Yes
Summary, means ± SD								
Focal	6 F/9 M	29.7 ± 9.6	51.9 ± 52.7	14.2 ± 9.5	55.9 ± 75.2	274.2 ± 92	387.8 ± 58.6	4 Yes | 11 No
GTCS	4 F/4 M	27 ± 5.9	86.3 ± 19.0	15.4 ± 11.2	96.3 ± 92.2	243.4 ± 108	412.8 ± 76.8	3 Yes | 5 No

Note that the latency of qT1 acquisition after the onset of the seizure was kept the same for interictal and postictal scans.
F = female; FS group = group of patients who had a focal seizure; GTCS group = group of patients who had a generalized tonic-clonic seizure; M = male.

clinical seizure-free period of at least 12 h. Seizure duration, injection latency, and seizure type were determined retrospectively based on the video-EEG recordings (see Tables 1 and 2 for details). Accordingly, patients were assigned to either the group of patients who had a secondary GTCS (GTCS group) or to the group of patients who had a focal seizure (FS group). The study was approved by the local Institutional Review Board and all patients provided written informed consent.

Seizure and injection of contrast agent

Gadolinium-based contrast agent causes a shortening of the T_1 time. A standard dose of 7.5 ml (1 mmol/ml) of the gadolinium-based contrast agent gadobutrol (Gadovist®) diluted with 40 ml saline solution was administered to the patient through a peripheral venous catheter. It was followed by 50 ml pure saline solution for flushing. The injection was performed by an automatic contrast injector (CT-Injektor Missouri™, ulrich medical) and was remotely initiated from the monitoring workstation where the onset of the seizure could be determined by means of EEG and video. After ictal injection, the patient was examined by a physician and transported to the MRI facility as soon as the clinical condition permitted. All patients were medically supervised by a physician during the transport to the MRI facility and the MRI scan. The interictal injection took place in the MRI facility.

Serum samples

Baseline serum samples of 37 patients were drawn at the onset of video-EEG monitoring, prior to the first recorded seizures as well as within the first 30 min after a seizure and 2, 6, 24 and 48 h after the index seizure. Seven of 37 patients were also participants of the imaging part of the current study. In five of 37 patients, a generalized seizure occurred during the timeframe described above. In these cases, a new set of serum sampling was started. Serum samples for MMP9 were stored at −80°C for later analysis using the Human MMP9 Quantikine ELISA Kit® (R&D Systems). Serum samples for S100 measurements were centrifuged at 4°C and processed within 48 h. S100 was measured with an electrochemiluminescence assay (ECLIA) on a cobas® e 411 modular analyzer (Roche Diagnostics) with the Elecsys® S100 reagent kit (Roche Diagnostics).

qT1 image acquisition and processing

Quantitative T_1 maps were acquired on a 3 T MAGNETOM Trio (Siemens Healthineers) using a 32-channel head receive coil and the scanner's body coil for radio frequency transmission. The optimized acquisition protocol was developed by

Table 2 Overview: clinical details

Patient ID	Structural MRI	Seizure description	Ictal EEG onset	Presumed SOZ
FS group				
1	Non-lesional	Sleep → arousal → tonic right arm elevation → bilateral tonic clonic	Obscured by muscle artefact	Left frontal
2	Incompletely resected FCD IIA in left parietal lobe	Sleep → vocalization, grimacing, dystonic arm posturing	Left central-parietal	Left parietal
3	Resected FCD IIA in left frontal lobe	Cough → vocalizations → behavioural arrest	Left temporal	Left temporal
4	Non-lesional	HV → déjà vu	Left temporal	Left temporal
5	Non-lesional	Sleep → arousal → movements with arm, rotational movements	Obscured by muscle/movement artefact	Right cingular
6	Subcortical heterotopia, mainly in right postcentral gyrus	Behavioural arrest	Right central temporal	Right central
7	Periventricular nodular heterotopia in left occipital lobe	Drowsy state → vocalizations → right tonic posturing → automatisms	Left temporal occipital	Left occipital
8	Resected cavernoma in left temporal lobe	HV → oral automatisms, behavioural arrest → manual automatisms	Left temporal	Left temporal
9	FCD in left precuneus	Behavioural arrest → oral automatisms, grimacing, right hand dystonia	Left central	Left precuneus
10	FCD in right frontal lob	Sleep → arousal → vocalization → body rocking	Right central	Right frontal
11	Non-lesional	Sleep → left hand dystonia → body rocking	Right central parietal	Right central
12	Non-lesional	Grimacing, oral automatisms, vocalization	Non-specific alpha/theta activity	Unknown
13	FCD in right temporal lobe	HV → behavioural arrest, dysphasia	Right temporal	Right temporal
14	FCD in left frontal lobe	body rocking, pedal automatisms	Obscured by muscle artifact	Left frontal
15	FCD in right frontal lobe	Vocalizations, rotation, hand automatisms	Obscured by muscle artefact	Right frontal
GTCS group				
16	FCD in right temporal and occipital lobe	behavioural arrest, oral automatisms	Right temporal	Right temporal/occipital
17	Non-lesional	Forced eye/head deviation to the right, sign of four with right arm extension to bilateral tonic clonic	Left frontal	Left frontal
18	Non-lesional	Sleep → arousal → rotation to the left → bilateral tonic clonic	Right frontal	Right frontal
19	Non-lesional	Sleep → tonic limb extension → left limb dystonia, right limb clonic movements	Generalized	Left frontal/parietal
20	Non-lesional	Left arm extension to symmetric limb extension, vocalization	Generalized/bifronto-central	Right frontal
21	FCD in left frontal lobe	Sleep → arousal → sign of 4 with right arm extension and left arm flexion → bilateral tonic clonic	Bifrontal	Left frontal
22	Multiple tubers, tuberous sclerosis	HV → behavioural arrest → vocalizations, head shaking → right hand automatisms → forced deviation to the left → bilateral tonic clonic	Right temporal	Right frontal
23	FCD in left frontal lobe	Forced head devotion to the right, left leg extension → bilateral tonic clonic	Bilateral frontal temporal	Left frontal
Summary				
Focal	7 FCD / 5 non-lesional / 2 heterotopia / 1 other			8 Left / 6 right / 1 unknown
GTCS	3 FCD / 4 non-lesional / 1 other			4 Left / 4 right

Note that the latency of qT1 acquisition after the onset of the seizure was kept the same for interictal and postictal scans.
FCD = focal cortical dysplasia; HV = hyperventilation; SOZ = seizure onset zone.

Preibisch and Deichmann (2009*a*, *b*). The basic processing steps of the qT1 data were performed using the FMRIB Software Library (FSL) (Smith *et al.*, 2004) and custom-built scripts written in MATLAB (MathWorks®). For detailed information see the online Supplementary material.

qT1 image analysis

Regions of interest analysis

Imaging data were analysed using FSL v5.0 (Smith *et al.*, 2004). First, pre-contrast volumes were skull-stripped, followed by an automated segmentation into three tissue classes (grey matter, white matter, CSF) using FMRIB's Automated Segmentation Tool (Zhang *et al.*, 2001; Smith, 2002). As accuracy of automated grey matter segmentation tools has been shown to greatly differ between datasets (Eggert *et al.*, 2012), visual quality control is crucial (Johnson *et al.*, 2017). Hence, all regions of interest were controlled visually for correct alignment. This was done by superimposing the regions of interest on the native qT1 volumes in native space and inspecting the intersection of the segmented regions of interest with the underlying MRI data. For each subject, postictal and interictal images were co-registered to the pre-contrast volume (Jenkinson *et al.*, 2002). To calculate the difference map (ΔqT1) indicating T_1 reduction upon contrast agent enhancement after epileptic seizures, postictal qT1 volumes were subtracted voxel-wise from the corresponding interictal qT1 volumes acquired with the same injection-to-qT1 latency. ΔqT1 values were averaged across all voxels belonging to the grey or the white matter mask, respectively, and taken for further analysis. Positive ΔqT1, thus, indicated contrast agent enhancement in the postictal as compared to the interictal qT1 volumes.

Voxel-wise analysis

The exact interindividual alignment is an essential factor in statistical group analyses of voxel-wise approaches. High degrees-of-freedom non-linear transformations are commonly used in spatial normalizations (Klein *et al.*, 2009). However, inaccuracies and misalignment, especially in cortical grey matter structures, can easily lead to misinterpretations of the underlying data and are subject to an ongoing debate in neuroimaging (Bookstein, 2001; Pruessner *et al.*, 2002; Smith *et al.*, 2006; Lerch *et al.*, 2017). To mitigate the effects of regional misalignment, spatially normalized images are typically smoothed via convolution with a 4–16 mm full-width at half-maximum Gaussian kernel. As discussed in the original publication by Smith *et al.* (2006), smoothing can increase sensitivity if the extent matches the size of the effect to be observed. However, as the spatial extent of postictal T_1 relaxation time differences is unknown, choosing an arbitrary size of a smoothing kernel may mask the effect of interest. Furthermore, qT1 values differ substantially between tissue types (white matter = 900 ms; grey matter = 1400 ms; CSF = 4500 ms), which renders effective partial voluming as crucial problem in statistical analyses. To circumvent the problems mentioned above, a TBSS (tract-based spatial statistics) inspired analysis was conducted (Smith *et al.*, 2006). While similar approaches have already been used in the analysis of diffusivity parameters (Ball *et al.*, 2013; Nazeri *et al.*, 2015), we here describe the usage of an adapted grey and white matter skeletonization procedure in the assessment of regional T_1 relaxation time differences. First, non-linear transformation warp fields to $1 \times 1 \times 1$ mm^3 MNI152 space were created for pre-contrast T_1-weighted volumes. These warp fields were in turn applied to individual partial volume estimates (PVEs), produced by FAST for grey and white matter, and to the ΔqT1 maps. To ensure cross-subject summation of postictal qT1 differences, all spatially normalized maps were flipped in *x*-direction for patients with the presumed seizure onset zone in the right hemisphere. The transformed PVEs were merged and averaged to create mean grey and white matter PVEs. The resulting mean PVEs were used for skeleton generation as described by Smith *et al.* (2006). In our adapted pipeline, the search direction perpendicular to the local grey or white matter surface was determined for every voxel in the image by finding the direction of biggest PVE probability change. By performing non-maximum suppression along the search direction, the mean PVEs were skeletonized to mostly 2D, curved surfaces containing only highly probable grey or white matter voxels, respectively. Local maxima of the spatially normalized individual PVEs were then projected onto the corresponding mean skeleton by searching again along the perpendicular direction for the most probable grey or white matter voxels. The resulting projection vectors were in turn used to fill the skeleton with the aligned ΔqT1 values for statistical analysis. Thereby, we broke down the individual whole-brain ΔqT1 maps to grey and white matter skeletons containing the qT1 differences from the most probable grey and white matter voxels, respectively, without the need of arbitrary smoothing and exact non-linear spatial alignment. See Fig. 1 for a schematic of data acquisition and analysis.

As this TBSS-like approach is experimental, all voxel-wise analyses were repeated applying a standard approach to ensure validity of our results: ΔqT1 maps were carefully normalized to the MNI152 template using the previously computed warp fields and minimally smoothed applying a 3D 2 mm Gaussian kernel. The resulting maps of increased contrast-enhancement spatially coincided with the clusters found in the above-described skeletonization approach, however, did not survive family-wise error (FWE) correction, most likely because of the discussed issue of effective partial voluming.

Statistical analysis

Regions of interest analysis

We used STATA 14.2 (StataCorp, College Station, TX) for region of interest analysis and analysis of biomarkers (see above). Accounting for repeated measurements, we used a mixed linear model to estimate and test various effects and interactions. The dependent variable was ΔqT1 and the independent variables were group (GTCS, FS) and injection-to-qT1 latency. The injection-to-qT1 latency was included in the model and controlled for as it highly varied between subjects and directly affects qT1. To yield robust results, we used a bootstrap analysis using 10 000 samples. For details of the statistical analysis of regions of interest see the online Supplementary material.

Voxel-wise analysis

Voxel-wise analysis was conducted using FSL's non-parametric Permutation Analysis of Linear Models (PALM) tool for permutation-based statistical inference (Winkler *et al.*, 2014, 2016). Here, we set up a two-group comparison, including

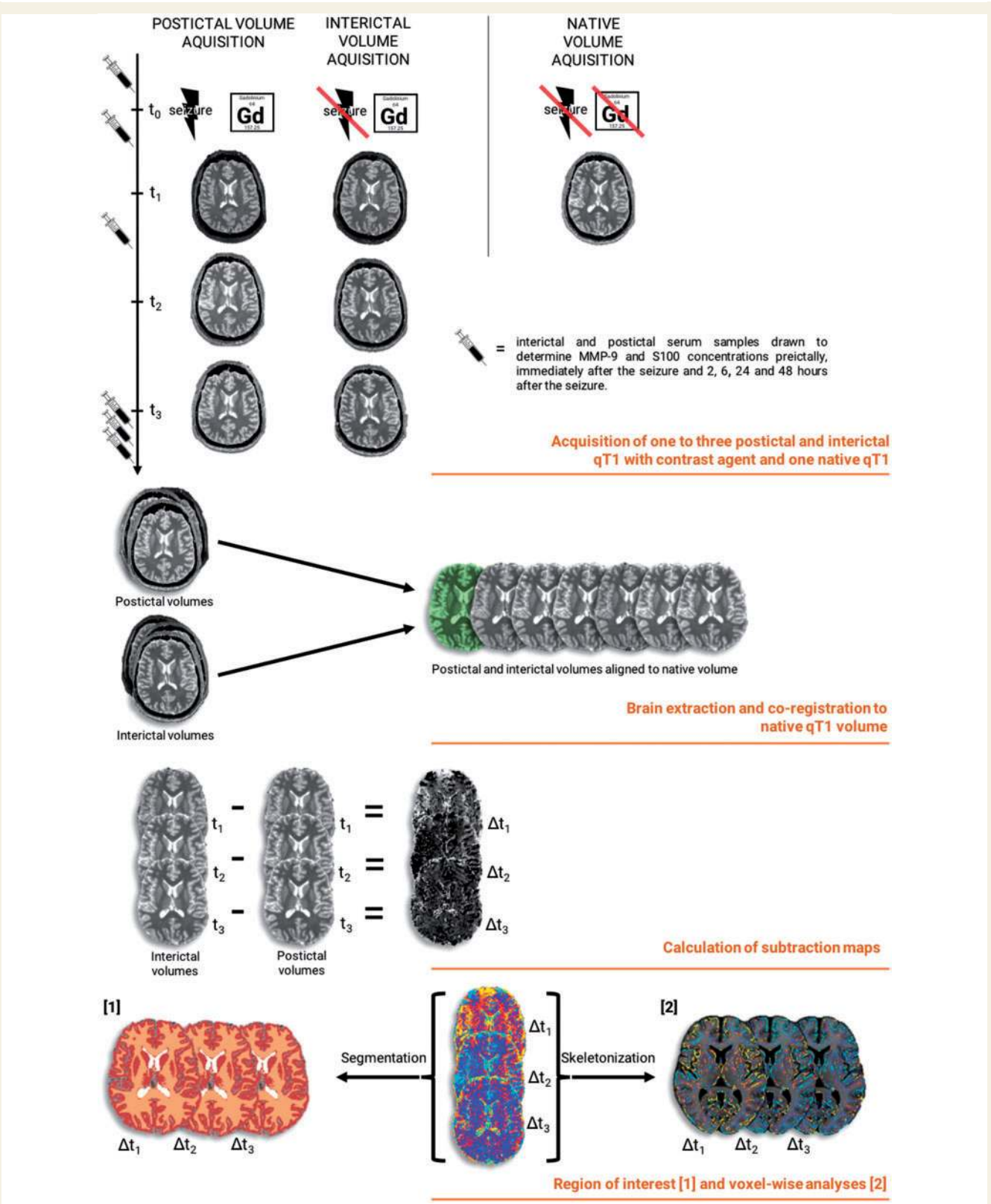

Figure 1 Schematic of data acquisition and preprocessing.

the demeaned injection-to-qT1 latency as continuous covariate, in which all scan time points were considered. This is achieved by defining exchangeability blocks restricting the permutations between groups on subjects with equal amount of measurements. For FWE correction we performed 2D threshold-free cluster enhancement due to the mostly 2D structure of

skeletonized imaging data. FWE-corrected clusters were considered significant at $P < 0.05$.

Statistical analysis of MMP9 and S100 serum

For the statistical analysis of MMP9 and S100 serum concentrations, we used a mixed linear model to estimate and test the influence of the time after the onset of the seizure on serum concentration of the respective marker. Results were confirmed by 10 000 bootstrappings.

Data availability

The data that support the findings of this study are available on request from the corresponding author. The data are not publicly available as they contain information that could compromise the privacy of research participants.

Results

Clinical group differences

Fifteen patients had secondary GTCS during video-EEG monitoring, whereas eight exhibited focal seizures (FS) only. The mean seizure duration was 51.9 s in the FS group and 86.3 s in the GTCS group ($t = -1.7$, df = 21, $P = 0.091$). Groups did not differ significantly in age ($t = 0.72$, df = 21, $P = 0.479$), gender ($\chi^2 = 0.21$, $P = 0.645$), number of scans ($t = -1.26$, df = 21, $P = 0.187$), latency of injection ($t = -0.27$, df = 21, $P = 0.788$), and in the injection-to-qT1 latency of the first scan ($t = -1.13$, df = 21, $P = 0.269$). The difference of the injection-to-qT1 latencies between the postictal and the interictal scans was below 8 min for all cases. Visual assessment of the first interictal scans by an expert neuroradiologist (E.H.) did not show any signs of interictal contrast enhancement. Details of the patient groups and of the measurements are provided in Tables 1 and 2.

Regions of interest ΔqT1 between-group differences

All 23 patients with epilepsy were considered for region of interest analysis. Of those, 16 were scanned more than once, resulting in 48 datasets that equally consisted of postictal and interictal volumes. The GTCS group showed a significantly higher ΔqT1 level in the whole-brain mask (i.e. lower T_1 in the postictal as compared to the interictal volumes) as compared to the FS group [GTCS > FS; mean difference ± standard error (SE): 35.97 ± 14.16 ms, 95% CI: 8.22–63.71 ms, $z = 2.54$, $P = 0.011$], when controlling for injection-to-qT1 latency. This whole-brain difference was further reflected by significantly higher ΔqT1 in global grey matter (32.68 ± 13.48 ms, 95% CI: 6.25–59.10 ms, $z = 2.42$; $P = 0.015$) and white matter (16.86 ± 8.37 ms, 95% CI: 0.45–33.25 ms, $z = 2.01$, $P = 0.044$) in the GTCS group as compared to the FS group, when controlling for injection-to-qT1 latency. Detailed descriptions of all region of interest results are given in Supplementary Table 1.

Voxel-wise ΔqT1 between-group differences

For voxel-wise analysis, one patient from the FS group had to be excluded, as the extent of their lesion negatively affected the robustness of the skeletonization process.

GTCS–FS group differences

Considering the full sample and including all scan time points adjusted for injection-to-qT1 latency, we observed widespread clusters indicating higher ΔqT1 in grey and white matter in the GTCS as compared to the FS group (GTCS > FS; uncorrected $P < 0.05$). Results maintained significance at a threshold of uncorrected $P < 0.001$, but are depicted here at a lower threshold for visualization purposes. The inverse contrast (GTCS < FS) did not yield any differences in ΔqT1 at a lenient uncorrected 5% significance threshold (Fig. 2).

Influence of injection-to-qT1 latency on ΔqT1 moderated by group

The effect of injection-to-qT1 latency on ΔqT1 is modified by the group effect (injection-to-qT1 latency × group interaction; FWE-corrected $P < 0.05$) specifically in the hemisphere contralateral to the presumed seizure onset zone. Here, the ΔqT1 decline is substantially faster in the GTCS groups as compared to the FS group (Fig. 3).

Early and late scans

To estimate the effect of injection-to-qT1 on ΔqT1, we divided our sample into two subsamples consisting of 'early' (injection-to-qT1 latency < 90 min, 12 FS versus six GTCS; EARLY subsample) and 'late' scans (injection-to-qT1 latency > 180 min, seven FS versus seven GTCS; LATE subsample). Both subsamples did not differ significantly in basic parameters (age, gender), whereas in the EARLY subsample, we observed significantly higher ΔqT1 in the GTCS group (GTCS > FS; uncorrected $P < 0.05$) in grey and white matter of both hemispheres as compared to the FS group (Fig. 4A). Results maintained significance at a threshold of uncorrected $P = 0.001$, but are depicted here at a lower threshold for visualization purposes. Analysis of the LATE subsample also revealed higher ΔqT1 in the GTCS group versus the FS group (GTCS > FS; FWE corrected $P < 0.05$), Here, differences were strictly lateralized to the hemisphere ipsilateral to the presumed seizure onset zone (Fig. 4B). The inverse contrasts (GTCS < FS) did not detect any significant results in both groups.

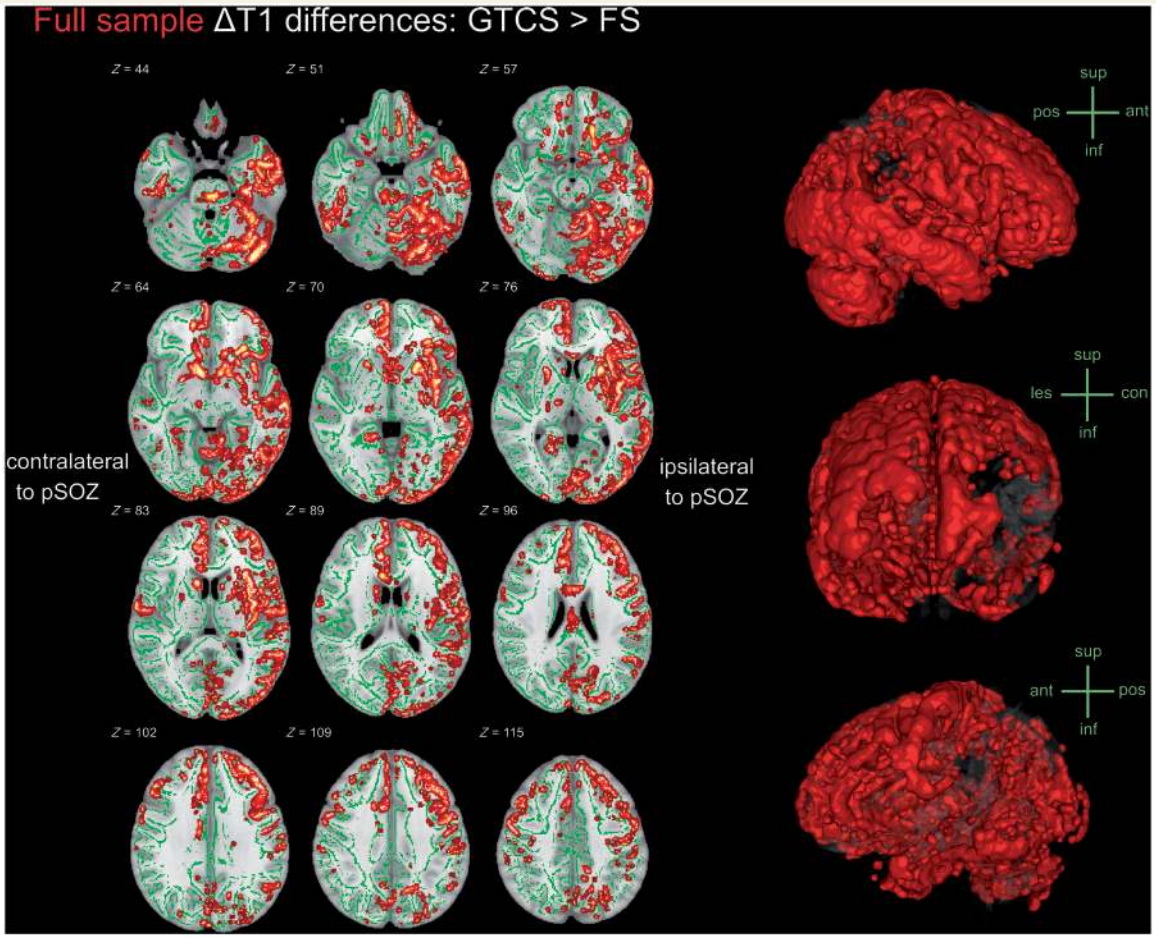

Figure 2 GTCS–FS group differences. *Left*: Hot colours indicate significantly higher ΔqT1 in all scan time points of the GTCS group as compared to all scan time points of the FS group (GTCS > FS; uncorrected $P < 0.05$). Results maintained statistical significance at a threshold of uncorrected $P < 0.001$, but are depicted here at a more lenient threshold for visualization purposes. Increases are displayed onto white and grey matter skeletons of the full sample (green). *Right*: Statistical images were rendered and visualized on the 3D volume of the MNI152 template. ant = anterior; inf = inferior; pos = posterior; pSOZ = presumed seizure onset zone; sup = superior.

Increased blood serum concentrations of postictal MMP9 and S100

S100 of 37 datasets and MMP9 of 27 datasets could be determined. Analyses were run separately for the GTCS (MMP9: $n = 21$; S100: $n = 31$) and the FS group (MMP9 and S100: $n = 6$). For both serum markers, the mixed linear model identified a significant main effect of the time after the onset of the seizure on blood serum levels in the GTCS group (MMP9: df = 5, $\chi^2 = 24.53$, $P = 0.0002$; S100: df = 5, $\chi^2 = 24.53$, $P = 0.0002$). MMP9 concentration was significantly elevated directly after the seizure (mean difference ± SE: 243.95 ± 89.04 ng/ml, 95% CI: 69.43–418.46 ng/ml, $z = 2.74$, $P = 0.006$). An increased level was still observed 2 h (265.06 ± 89.04 ng/ml, 95% CI: 90.54–439.57 ng/ml, $z = 2.98$, $P = 0.003$) and 6 h (358.34 ± 89.04 ng/ml, 95% CI: 183.82–532.86 ng/ml, $z = 4.02$, $P < 0.001$) after seizure (Fig. 5A). S100 blood serum concentrations were significantly elevated directly after the seizure (mean difference ± SE: 0.05 ± 0.01 µg/l, 95% CI: 0.03–0.07 µg/l, $z = 4.28$, $P < 0.001$) but dropped to baseline 2 h afterwards (SE: 0.01 ± 0.01 µg/l, 95% CI: 0.03–0.03 µg/l, $z = 1.03$, $P = 0.304$) (Fig. 5B). In the FS group, both MMP9 and S100 showed similar trends, but differences did not reach statistical significance. Detailed information of pairwise comparisons and confidence intervals can be found in Supplementary Table 2.

Discussion

This study yields two main findings. First, blood–brain barrier dysfunction in epilepsy is temporally (Hypothesis 1) and anatomically (Hypothesis 2) associated with epileptic seizures. Second, this ictally-associated blood–brain barrier dysfunction may be measured by a new quantitative MRI protocol, which contrasts volumes resulting from T_1-relaxometry after both ictal and interictal injection of gadolinium-based contrast agent.

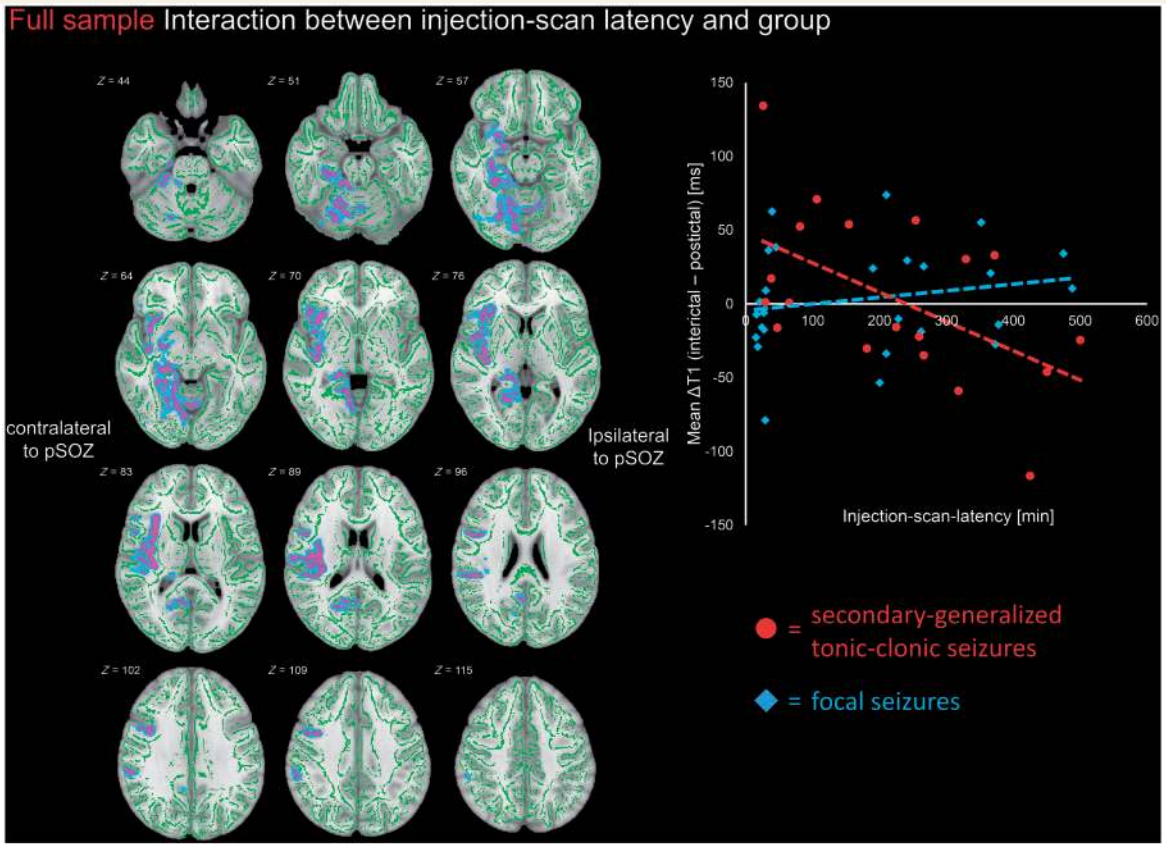

Figure 3 Influence of injection-to-qT1 latency on ΔqT1 moderated by group (GTCS/FS). Cool colours indicate where the effect of injection-to-qT1 latency on ΔqT1 is modified by group (FWE-corrected $P < 0.05$). Results are superimposed on the white and grey matter skeleton of the full sample (green). The graph shows exemplary mean ΔqT1 values of the grey matter cluster in each interictal-postictal dataset of all patients plotted against the respective injection-to-qT1 latency. pSOZ = presumed seizure onset zone.

ΔqT1 as functional imaging marker

Our imaging protocol allowed us to scrutinize what has been termed 'transient postictal MRI signal changes' (Yaffe *et al.*, 1995; Hattingen *et al.*, 2008; Cianfoni *et al.*, 2013). These signal changes may reflect altered perfusion, oedema, and blood–brain barrier dysfunction. Here, we sensitized our MRI protocol to alterations in vascular integrity after injection of gadolinium-based contrast agent. Quantitative T_1-mapping applied in the current study has been proven to be even more sensitive in the detection of contrast agent enhancement than conventional MRI (Hattingen *et al.*, 2013; Jurcoane *et al.*, 2013; Bourcier *et al.*, 2017). By comparing postictal to interictal quantitative volumes, subtle extravascular enhancements of contrast agent shall, thus, be detected. Also, intravascular contrast agent is detected, which influences ΔqT1 in case of postictal alterations in perfusion. Hypoperfusion has been described to occur postictally (Leonhardt *et al.*, 2005; Von Oertzen *et al.*, 2011; Gaxiola-Valdez *et al.*, 2017), leading to potentially less contrast agent in the postictal as compared to the interictal scans. Our results, however, are indicative of more contrast agent in the postictal as compared to the interictal scans. Thus, it appears likely that positive ΔqT1 stems from extravascular (as opposed to intravascular) contrast agent. The fact that positive ΔqT1 is found several hours after the onset of seizure points in the same direction (see next paragraph). It should be noted that the results of the full sample and the early subsample (Figs 2 and 4A) in contrast to the results of the interaction analysis and the late subsample (Figs 3 and 4B) do not survive correction for multiple comparison. Therefore, caution is warranted when interpreting them, and our claims are more firmly substantiated by the FWE-corrected results. The reason for the full sample and the early subsample results not surviving correction for multiple comparison may lie in the signal alteration of qT1 by postictal hypoperfusion increasing the statistical spread of data in the between-groups tests. It is known that postictal hypoperfusion normalizes after more than 90 min (Gaxiola-Valdez *et al.*, 2017).

Temporal seizure-association of ΔqT1: Hypothesis 1

Transient postictal MRI signal changes have been described minutes to hours after the seizure (Cianfoni *et al.*, 2013).

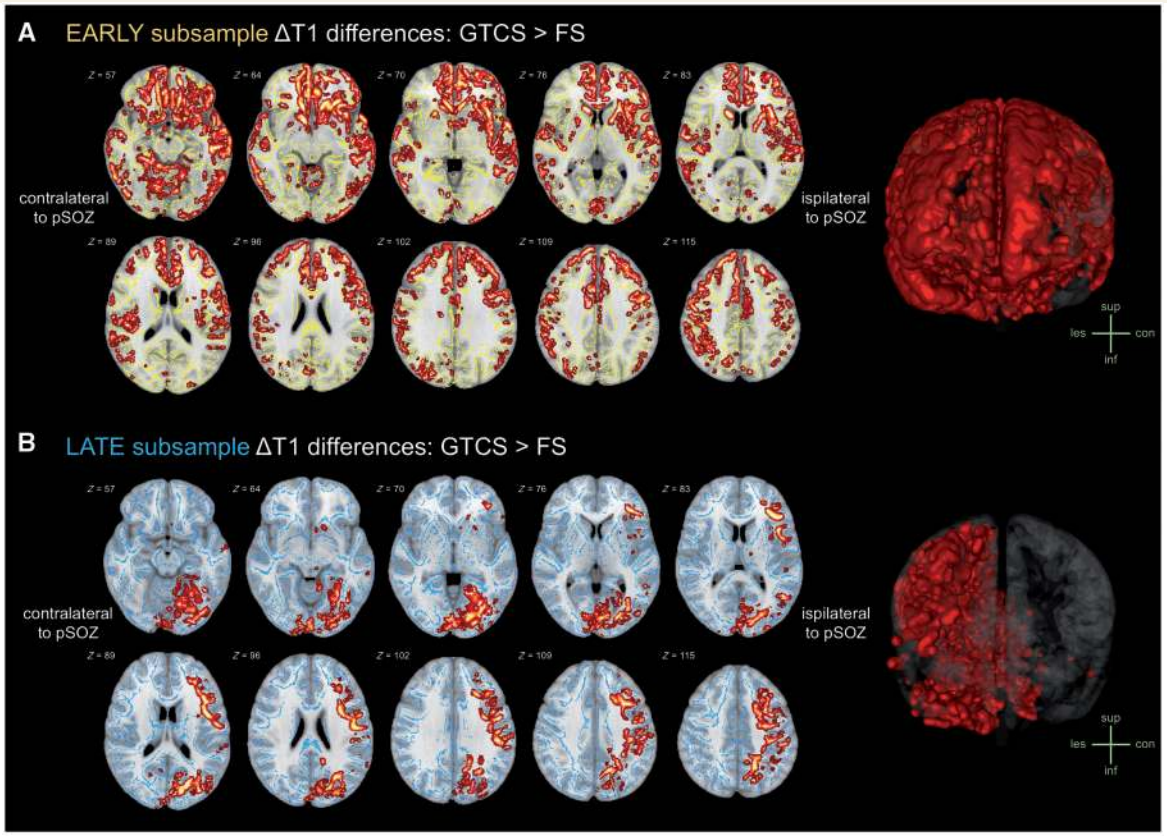

Figure 4 Early and late scans. (**A**) The early subsample shows significantly higher ΔqT1 (hot colours) in both hemispheres of the GTCS group as compared to the FS group (GTCS > FS; uncorrected $P < 0.05$). Results maintained statistical significance at a threshold of uncorrected $P < 0.001$, but are depicted here at a more lenient threshold for visualization purposes. (**B**) Supra-threshold voxels of the same contrast in the late subsample are only found in the hemisphere ipsilateral to the presumed seizure onset zone (GTCS > FS; FWE-corrected $P < 0.05$). Corresponding results are displayed on the white and grey matter skeleton of the early (yellow) and late (blue) subsample. Statistical images were rendered and visualized on the 3D volume of the MNI152 template. con = contralesional hemisphere; inf = inferior; les = lesional hemisphere; pSOZ = presumed seizure onset zone; sup = superior.

A recent study could clearly delineate postictal hypoperfusion by means of arterial spin labelling in the vicinity of the seizure onset zone (Gaxiola-Valdez *et al.*, 2017) up to 90 min after the seizure. In the current study, we found higher ΔqT1 in the GTCS group as compared to the FS group more than 180 min after ictal injection. This corroborates our interpretation of ΔqT1 as indicator of (extravascular) enhancement of contrast agent. Furthermore, clusters appeared to be more delineated in the hemisphere ipsilateral to the presumed seizure onset zone in later as compared to earlier scans (Fig. 4). Possibly, this reflects the effect of postictal hypoperfusion normalizing more than 90 min after seizure onset. The injection-to-qT1 latency × group interaction needs additional mentioning: interestingly, it is specifically observed in the hemisphere contralateral to the presumed seizure onset zone thought to be only compromised by ictal epileptic activity in the GTCS group. Here ΔqT1 decays as a function of time, whereas it does not in the FS group, in which seizure activity was restricted to the hemisphere ipsilateral to the presumed seizure onset zone. We believe this to be a washout effect of extravascular contrast agent indicating contralateral blood–brain barrier dysfunction only in the GTCS group. The serum concentration of gadolinium has been shown to halve within 3.5 h (Aime *et al.*, 2009) in healthy subjects. Despite this relatively short plasma elimination half-life, the finding of significant between-group differences more than 180 min after seizure onset leaves a large time window for the detection of postictal gadolinium enhancement in grey matter. However, it should be clearly stated that the onset of the postictal blood–brain barrier dysfunction may not exactly be defined by the imaging part of the current study. All injections have started a minimum of 14 s and on average 49.3 s (SD: 40.1) before the end of the seizure (Table 1). Based on dynamic contrast-enhanced MRI, we know that it takes 5–10 s before the contrast agent reaches the brain following injection to a peripheral vein. We, thus, assume that gadolinium accumulates in the ictal brain in all cases. However, blood–brain barrier dysfunction could occur during the seizure or at any time

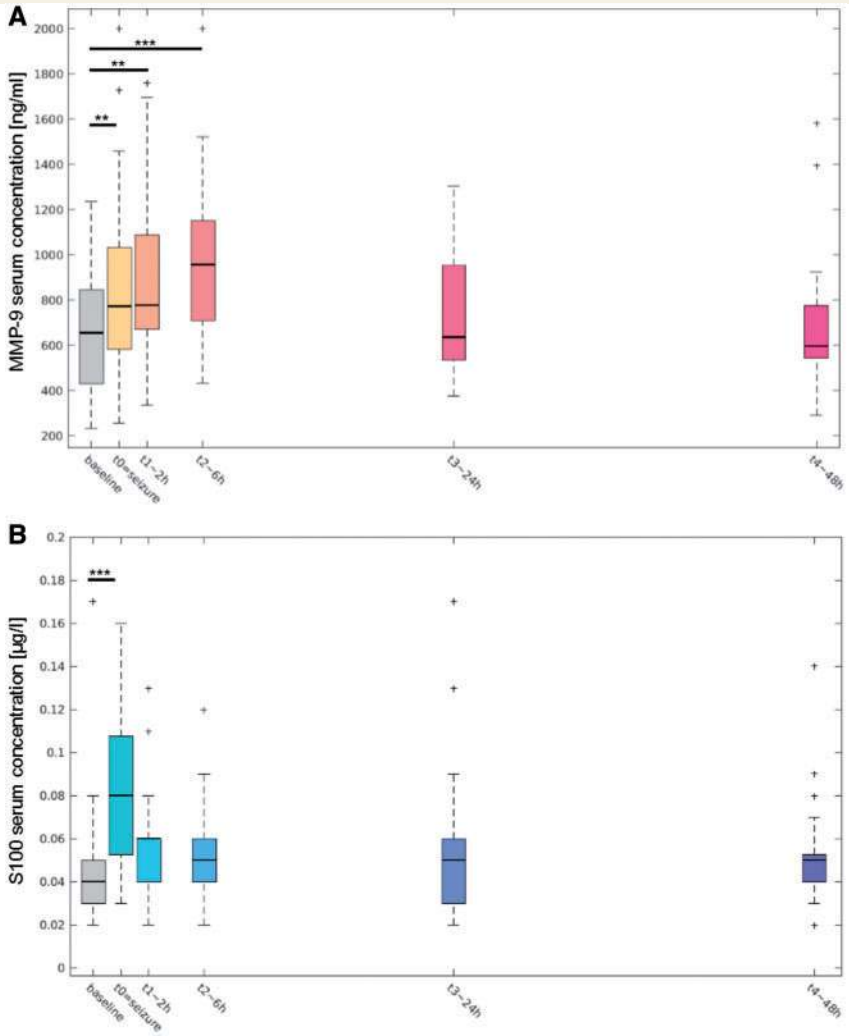

Figure 5 Blood serum biomarker analysis. Blood serum concentrations of (**A**) MMP9 (ng/ml) and (**B**) S100 (µg/l) as a function of time post-onset of the seizure in the GTCS group. Boxplots display the sample mean and extend from 25th to 75th percentile. Whiskers correspond to approximately ± 2.7 SD. Asterisks indicate significance of pairwise comparisons based on mixed model. $^{**}P < 0.01$, $^{***}P < 0.001$.

postictally before qT1 acquisition. The analysis of serum markers is more informative in this regard as it shows a direct postictal increase of S100 serum levels and, thus, in accordance with results of animal studies (Vazana *et al.*, 2016), indicates an immediate postictal blood–brain barrier affection. The contrast of postictally and interictally acquired scans ensures that only transient and ictally-associated alterations of blood–brain barrier permeability will be imaged. Epileptogenic lesions are known to exhibit signs of permanent/interictal blood–brain barrier dysfunction (Marchi *et al.*, 2012). These could not be demonstrated by visual expert assessment of interictal volumes in the current sample, which, however, is not as sensitive as quantitative analysis. It is, thus, important to note that additional to the peri-ictal blood–brain barrier dysfunction found here, interictal blood–brain barrier dysfunction may occur.

Anatomical seizure-association of ΔqT1: Hypothesis 2

By comparing patients with GTCS to patients with FS, we aimed to test the hypothesis that postictal blood–brain barrier dysfunction is directly linked to the anatomical spread of ictal epileptic activity. Whereas focal seizures compromise variant anatomical parts of the hemisphere ipsilateral to the presumed seizure onset zone, secondarily generalized tonic-clonic seizures are thought to affect both hemispheres. Correspondingly, clusters indicating between-group differences in ΔqT1 are found globally. Clusters indicating scan-latency × group interaction and late between-group differences in ΔqT1 (Figs 3 and 4B) are strictly located in the hemispheres contralateral and ipsilateral to the presumed seizure onset zone, respectively, most likely indicating preceding ictal epileptic activity in the GTCS as

compared to the FS group. It is subject to our ongoing studies to show whether these effects also persist on an individual level and can, thereby, be used to localize the seizure onset zone in a diagnostic setting. When using the TBSS-like approach for individual-level analysis, maximal contrast agent enhancement was found in the vicinity of the presumed seizure onset zone in some cases (Fig. 6A), whereas no region of maximal contrast agent enhancement could be found in other cases (Fig. 6B). At this state, it is unclear which factors determine whether contrast agent enhancement reflecting ictal activity can be used to delineate the presumed seizure onset zone. Importantly, maximal contrast agent enhancement could be found in the vicinity of the presumed seizure onset zone in a non-lesional patient (Patient 1 in Fig. 6). It is obvious that magnetic resonance-negative patients would particularly benefit from an imaging protocol geared towards visualizing ictal activity instead of epileptogenic lesions.

S100 and MMP9 as serum markers

Increased postictal serum levels of S100 and MMP9 corroborate our interpretation of between-group differences in ΔqT1 as indicative of blood–brain barrier dysfunction. Furthermore, they replicate the results of previous studies (Kapural *et al.*, 2002; Li *et al.*, 2013; Ljubisavljevic *et al.*, 2015). The early increase of S100 observed minutes after the seizure is a strong argument that the contrast agent enhancement seen in MRI relates to a blood–brain barrier dysfunction occurring during the seizure or shortly after. Of note, this is not contradicted by the delayed increase of MPP9, which is known to reflect blood–brain barrier dysfunction only hours after it occurred (Li *et al.*, 2013). Most interestingly, a recent animal study has found MMP to play a functional role in the mediation of peri-ictal blood–brain barrier dysfunction (Rempe *et al.*, 2018).

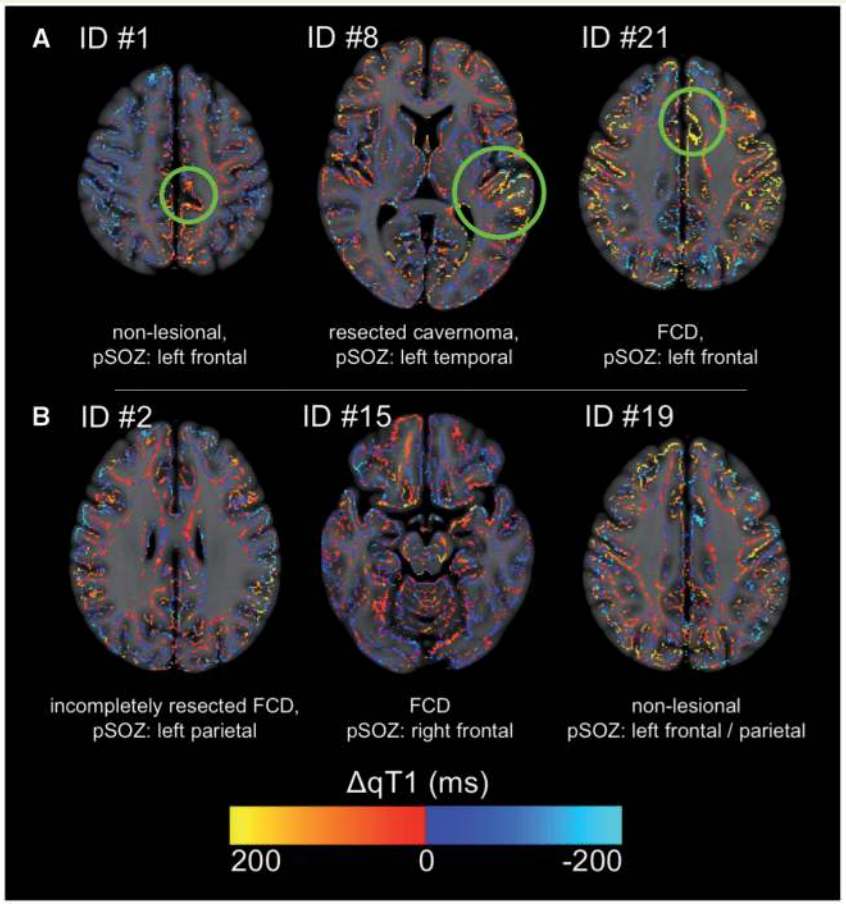

Figure 6 Individual-level results of six representative cases. The TBSS-like approach applied for group-wise testing was used for individual-level analysis. The latest scans acquired from each subject were taken for individual-level analysis as the influence of post-ictal perfusion was believed to be reduced or absent in these scans. The presumed seizure onst zone (pSOZ) is delineated by green circles in cases in which it co-localizes with a visually determined zone of maximal contrast agent enhancement. (**A**) Three exemplary cases in which maximal contrast agent enhancement coincides with presumed seizure onset zone. (**B**) Three exemplary cases without region of maximal contrast agent enhancement. It should be noted that Patient 1 is non-lesional according to data derived from 3 T MRI. Also, Patients 19 and 21, who exhibited secondary generalized tonic-clonic seizures, show more global enhancement of contrast agent as compared to Patients 1, 2, 15 and 8, who exhibited focal seizures and show focal enhancement of contrast agent. FCD = focal cortical dysplasia; pSOZ = presumed seizure onset zone.

Conclusion and outlook

The current study provides evidence for the occurrence of a blood–brain barrier dysfunction that is temporally (Hypothesis 1) and anatomically (Hypothesis 2) associated with epileptic seizures. Quantitative T_1 after ictal contrast agent injection is shown to be a valuable imaging marker of peri-ictal blood–brain barrier dysfunction several hours after onset of the seizure. However, to date it is unclear whether these measurements will also be successful on an individual level. Nonetheless, the current study could be a first stepping stone on the way to complement epilepsy imaging by seizure imaging. Future studies may be able to *post hoc* measure ictally-associated blood–brain barrier dysfunction in individual patients, thereby visualizing the traces of single epileptic seizures and localizing their origin (Rüber *et al.*, 2018). The imaging protocol introduced in this study could, thereby, become a diagnostic modality in presurgical evaluation of epilepsy patients, where it would be of particular importance for non-lesional epilepsy patients. A better understanding of the peri-ictal blood–brain barrier dysfunction may, furthermore, inspire novel therapies exploiting peri-ictal drug infusion (Henshall *et al.*, 2016; Vazana *et al.*, 2016) for enhanced focal drug delivery in brain regions affected by epilepsy.

Acknowledgements

The authors thank Maria Schruff and her team from the Video-EEG monitoring unit at the Bonn Department of Epileptology (University of Bonn Medical Center, Bonn, Germany) whose help has been indispensable for the current study. They, furthermore, thank the other members of the junior research group for translational neuroimaging at the Bonn Department of Epileptology, namely, Jennifer Gaubatz, Jasmine Eberle, Carolina Vargas, Leon Ernst and Conrad Prillwitz, for critical comments. They thank Laura Schinabeck (University of Bonn, Bonn, Germany) for technical assistance in data acquisition. Lastly, the authors are grateful for the kind support provided by the Verein zur Förderung der Epilepsieforschung e.V.

Funding

Funded by the BONFOR research commission of the medical faculty of the University of Bonn (2017-6-02).

Competing interests

The authors report no competing interests.

Supplementary material

Supplementary material is available at *Brain* online.

References

Aime S, Caravan P. Biodistribution of gadolinium-based contrast agents, including gadolinium deposition. J Magn Reson Imaging 2009; 30: 1259–67.

Alvarez V, Maeder P, Rossetti AO. Postictal blood-brain barrier breakdown on contrast-enhanced MRI. Epilepsy Behav 2010; 17: 302–3.

Ball G, Srinivasan L, Aljabar P, Counsell SJ, Durighel G, Hajnal J V, et al. Development of cortical microstructure in the preterm human brain. Proc Natl Acad Sci USA 2013; 110: 9541–6.

Bar-Klein G, Lublinsky S, Kamintsky L, Noyman I, Veksler R, Dalipaj H, et al. Imaging blood–brain barrier dysfunction as a biomarker for epileptogenesis. Brain 2017; 140: 1692–705.

Barr TL, Latour LL, Lee K-Y, Schaewe TJ, Luby M, Chang GS, et al. Blood-brain barrier disruption in humans is independently associated with increased matrix metalloproteinase-9. Stroke 2010; 41: e123–8.

Bookstein FL. 'Voxel-based morphometry' should not be used with imperfectly registered images. Neuroimage 2001; 14: 1454–62.

Bourcier R, Brecheteau N, Costalat V, Daumas-Duport B, Guyomarch-Delasalle B, Desal H, et al. MRI quantitative T2* mapping on thrombus to predict recanalization after endovascular treatment for acute anterior ischemic stroke. J Neuroradiol 2017; 44: 241–6.

Cianfoni A, Caulo M, Cerase A, Della Marca G, Falcone C, Di Lella GM, et al. Seizure-induced brain lesions: a wide spectrum of variably reversible MRI abnormalities. Eur J Radiol 2013; 82: 1964–72.

Deoni SC. Quantitative relaxometry of the brain. Top Magn Reson Imaging 2010; 21: 101–13.

Eggert LD, Sommer J, Jansen A, Kircher T, Konrad C. Accuracy and reliability of automated gray matter segmentation pathways on real and simulated structural magnetic resonance images of the human brain. PLoS One 2012; 7: e45081.

Fieschi C, Lenzi GL, Zanette E, Orzi F, Passero S. Effects on EEG of the osmotic opening of the blood-brain barrier in rats. Life Sci 1980; 27: 239–43.

Friedman A. Blood-brain barrier dysfunction, status epilepticus, seizures and epilepsy: a puzzle of a chicken and egg? Epilepsia 2012; 52: 19–20.

Gaxiola-Valdez I, Singh S, Perera T, Sandy S, Li E, Federico P. Seizure onset zone localization using postictal hypoperfusion detected by arterial spin labelling MRI. Brain 2017; 140: 2895–911.

Hattingen E, Jurcoane A, Daneshvar K, Pilatus U, Mittelbronn M, Steinbach JP, et al. Quantitative T2 mapping of recurrent glioblastoma under bevacizumab improves monitoring for non-enhancing tumor progression and predicts overall survival. Neuro Oncol 2013; 15: 1395–404.

Hattingen E, Jurcoane A, Nelles M, Müller A, Nöth U, Mädler B, et al. Quantitative MR imaging of brain tissue and brain pathologies. Clin Neuroradiol 2015; 25: 219–24.

Hattingen E, Raab P, Lanfermann H, Zanella FE, Weidauer S. Postiktale MR-Veränderungen. Radiologe 2008; 48: 1058–65.

Henshall DC, Hamer HM, Pasterkamp RJ, Goldstein DB, Kjems J, Prehn JHM, et al. MicroRNAs in epilepsy: pathophysiology and clinical utility. Lancet Neurol 2016; 15: 1368–76.

Horowitz SW, Merchut M, Fine M, Azar-Kia B. Complex partial seizure-induced transient MR enhancement. J Comput Assist Tomogr 1992; 16: 814–16.

Ivens S, Kaufer D, Flores LP, Bechmann I, Zumsteg D, Tomkins O, et al. TGF-β receptor-mediated albumin uptake into astrocytes is involved in neocortical epileptogenesis. Brain 2007; 130: 535–47.

Jasper HH. Physiopathological mechanisms of post-traumatic epilepsy. Epilepsia 1970; 11: 73–80.

Jenkinson M, Bannister P, Brady M, Smith S. Improved optimization for the robust and accurate linear registration and motion correction of brain images. Neuroimage 2002; 17: 825–41.

Johnson EB, Gregory S, Johnson HJ, Durr A, Leavitt BR, Roos RA, et al. Recommendations for the use of automated gray matter segmentation tools: evidence from Huntington's disease. Front Neurol 2017; 8: 519.

Jurcoane A, Wagner M, Schmidt C, Mayer C, Gracien R-M, Hirschmann M, et al. Within-lesion differences in quantitative MRI parameters predict contrast enhancement in multiple sclerosis. J Magn Reson Imaging 2013; 38: 1454–61.

Kapural M, Krizanac-Bengez L, Barnett G, Perl J, Masaryk T, Apollo D, et al. Serum S-100b as a possible marker of blood–brain barrier disruption. Brain Res 2002; 940: 102–4.

Klein A, Andersson J, Ardekani BA, Ashburner J, Avants B, Chiang M-C, et al. Evaluation of 14 nonlinear deformation algorithms applied to human brain MRI registration. Neuroimage 2009; 46: 786–802.

Lerch JP, van der Kouwe AJW, Raznahan A, Paus T, Johansen-Berg H, Miller KL, et al. Studying neuroanatomy using MRI. Nat Neurosci 2017; 20: 314–26.

Leonhardt G, De Greiff A, Weber J, Ludwig T, Wiedemayer H, Forsting M, et al. Brain perfusion following single seizures. Epilepsia 2005; 46: 1943–9.

Li YJ, Wang ZH, Zhang B, Zhe X, Wang MJ, Shi ST, et al. Disruption of the blood-brain barrier after generalized tonic-clonic seizures correlates with cerebrospinal fluid MMP-9 levels. J Neuroinflammation 2013; 10: 80.

Librizzi L, Noè F, Vezzani A, De Curtis M, Ravizza T. Seizure-induced brain-borne inflammation sustains seizure recurrence and blood-brain barrier damage. Ann Neurol 2012; 72: 82–90.

Ljubisavljevic S, Stojanovic I, Basic J, Vojinovic S, Stojanov D, Djordjevic G, et al. The role of matrix metalloproteinase 3 and 9 in the pathogenesis of acute neuroinflammation. implications for disease modifying therapy. J Mol Neurosci 2015; 56: 840–7.

Marchi N, Granata T, Ghosh C, Janigro D. Blood-brain barrier dysfunction and epilepsy: pathophysiologic role and therapeutic approaches. Epilepsia 2012; 53: 1877–86.

Margaret Cheng H-L, Stikov N, Ghugre NR, Wright GA. Practical medical applications of quantitative MR relaxometry. J Magn Reson Imaging 2012; 36: 805–24.

Nazeri A, Chakravarty MM, Rotenberg DJ, Rajji TK, Rathi Y, Michailovich OV, et al. Functional consequences of neurite orientation dispersion and density in humans across the adult lifespan. J Neurosci 2015; 35: 1753–62.

Obermeier B, Daneman R, Ransohoff RM. Development, maintenance and disruption of the blood-brain barrier. Nat Med 2013; 19: 1584–96.

Preibisch C, Deichmann R. Influence of RF spoiling on the stability and accuracy of T1 mapping based on spoiled FLASH with varying flip angles. Magn Reson Med 2009a; 61: 125–135.

Preibisch C, Deichmann R. T1 mapping using spoiled FLASH-EPI hybrid sequences and varying flip angles. Magn Reson Med 2009b; 62: 240–6.

Pruessner JC, Köhler S, Crane J, Pruessner M, Lord C, Byrne A, et al. Volumetry of temporopolar, perirhinal, entorhinal and parahippocampal cortex from high-resolution MR images: considering the variability of the collateral sulcus. Cereb Cortex 2002; 12: 1342–53.

Rempe RG, Hartz AMS, Soldner ELB, Sokola BS, Alluri SR, Abner EL, et al. Matrix metalloproteinase-mediated blood-brain barrier dysfunction in epilepsy. J Neurosci 2018; 38: 4301–5.

Roch C, Leroy C, Nehlig A, Namer IJ. Magnetic resonance imaging in the study of the lithium-pilocarpine model of temporal lobe epilepsy in adult rats. Epilepsia 2002; 43: 325–35.

Rüber T, David B, Elger CE. MRI in epilepsy: clinical standard and evolution. Curr Opin Neurol 2018; 31: 223–31.

Seiffert E, Dreier JP, Ivens S, Bechmann I, Tomkins O, Heinemann U, et al. Lasting blood—brain barrier disruption induces epileptic focus in the rat somatosensory cortex. Neurobiol Dis 2004; 24: 7829–36.

Smith SM. Fast robust automated brain extraction. Hum Brain Mapp 2002; 17: 143–55.

Smith SM, Jenkinson M, Johansen-Berg H, Rueckert D, Nichols TE, Mackay CE, et al. Tract-based spatial statistics: voxelwise analysis of multi-subject diffusion data. Neuroimage 2006; 31: 1487–505.

Smith SM, Jenkinson M, Woolrich MW, Beckmann CF, Behrens TEJ, Johansen-Berg H, et al. Advances in functional and structural MR image analysis and implementation as FSL. Neuroimage 2004; 23: S208–19.

Vazana U, Veksler R, Pell GS, Prager O, Fassler M, Chassidim Y, et al. Glutamate-mediated blood-brain barrier opening: implications for neuroprotection and drug delivery. J Neurosci 2016; 36: 7727–39.

van Vliet EA, Otte WM, Gorter JA, Dijkhuizen RM, Wadman WJ. Longitudinal assessment of blood–brain barrier leakage during epileptogenesis in rats. A quantitative MRI study. Neurobiol Dis 2014; 63: 74–84.

van Vliet EA, Otte WM, Wadman WJ, Aronica E, Kooij G, de Vries HE, et al. Blood-brain barrier leakage after status epilepticus in rapamycin-treated rats I: magnetic resonance imaging. Epilepsia 2016; 57: 59–69.

Von Oertzen TJ, Mormann F, Urbach H, Reichmann K, Koenig R, Clusmann H, et al. Prospective use of subtraction ictal SPECT coregistered to MRI (SISCOM) in presurgical evaluation of epilepsy. Epilepsia 2011; 52: 2239–48.

Weissberg I, Wood L, Kamintsky L, Vazquez O, Milikovsky DZ, Alexander A, et al. Albumin induces excitatory synaptogenesis through astrocytic TGF-β/ALK5 signaling in a model of acquired epilepsy following blood-brain barrier dysfunction. Neurobiol Dis 2015; 78: 115–25.

Winkler AM, Ridgway GR, Douaud G, Nichols TE, Smith SM. Faster permutation inference in brain imaging. Neuroimage 2016; 141: 502–16.

Winkler AM, Ridgway GR, Webster MA, Smith SM, Nichols TE. Permutation inference for the general linear model. Neuroimage 2014; 92: 381–97.

Yaffe K, Ferriero D, Barkovich a J, Rowley H. Reversible MRI abnormalities following seizures. Neurology 1995; 45: 104–8.

Zappulla RA, Spigelman MK, Omsberg E, Rosen JJ, Malis LI, Holland JF. Electroencephalographic consequences of sodium dehydrocholate-induced blood-brain barrier disruption: part 1. Acute and chronic effects of intracarotid sodium dehydrocholate. Neurosurgery 1985a; 16: 630–8.

Zappulla RA, Spigelman MK, Rosen JJ, Marotta D, Malis LI, Holland JF. Electroencephalographic consequences of sodium dehydrocholate-induced blood-brain barrier disruption: part 2. Generation and propagation of spike activity after the topical application of sodium dehydrocholate. Neurosurgery 1985b; 16: 639–43.

Zhang Y, Brady M, Smith S. Segmentation of brain MR images through a hidden Markov random field model and the expectation-maximization algorithm. IEEE Trans Med Imaging 2001; 20: 45–57.